Cardiovascular Diabetology

https://doi.org/10.1186/s12933-026-03329-3

Article in Press

Unmasking subclinical cardiac dysfunction in type 2 diabetes through genetic and epigenetic profiling

Received: 13 May 2026

Accepted: 1 August 2026

Published online: 17 August 2026

Cite this article as: Primio C., Hafeez K.S., Casalone E. *et al.* Unmasking subclinical cardiac dysfunction in type 2 diabetes through genetic and epigenetic profiling. *Cardiovasc Diabetol* (2026). https://doi.org/10.1186/s12933-026-03329-3

Cecilia Primio, Khadija Sana Hafeez, Elisabetta Casalone, Rebecca Filomena, Miriam Rosselli, Alessia Russo, Alessandra Allione, Simonetta Guarrera, Bianca Riccardi, Paul Balfanz, Bart Jacobs, Yvan Devaux, Javier Bermejo, Stephane Heymans, Benedicte Gaborit, Cyrille Bergerot, Florian Sohler, Robin Liechti, Olivier Martin, Josefina Lascano-Maillard, Mark Ibberson, Étienne Audureau, Rui Wang-Sattler, Chim C. Lang, Flora Sam, Geneviève Derumeaux, Giuseppe Matullo & Cardiateam Consortium

Unmasking Subclinical Cardiac Dysfunction in Type 2 Diabetes Through Genetic and Epigenetic Profiling

Cecilia Di Primio[a] † MSc, Khadija Sana Hafeez[a] † PhD, Elisabetta Casalone[a] PhD, Rebecca Filomena[a] MSc, Miriam Rosselli[a] MSc, Alessia Russo[a] PhD, Alessandra Allione[a] PhD, Simonetta Guarrera[a,b] MSc, MPH, Bianca Riccardi[c,d] MSc, Paul Balfanz[c,e,f] MD, Bart Jacobs[g] MD, Yvan Devaux[h] PhD, Javier Bermejo[i] MD, PhD, Stephane Heymans[j,k,l] MD, PhD, Benedicte Gaborit[m,n] MD, PhD, Cyrille Bergerot[o] MD, Florian Sohler[p] PhD, Robin Liechti[q] PhD, Olivier Martin[q] MSc, Josefina Lascano Maillard[q] PhD, Mark Ibberson[q] PhD, Étienne Audureau[c,d] MD, PhD, Rui Wang-Sattler[r] PhD, Chim C Lang[s] MD, Flora Sam[t,u] MD, Geneviève A Derumeaux[c,e] * MD, PhD, Giuseppe Matullo[a,v] * PhD, On behalf of Cardiateam Consortium

a) University of Turin, Unit of Genomic Variability and Complex Diseases, Department of Medical Sciences, Turin, Italy
b) Italian Institute for Genomic Medicine (IIGM), FPO Istituto di Ricovero e Cura a Carattere Scientifico - I.R.C.C.S., Candiolo, Italy
c) Université Paris-Est Créteil, INSERM, IMRB, FHU Senec, Créteil, France
d) Henri Mondor Hospital, Assistance Publique Hôpitaux de Paris, Biostatistics Department, Créteil, France
e) Henri Mondor Hospital, Assistance Publique Hôpitaux de Paris, Département de Physiologie-Explorations Fonctionnelles, Créteil, France
f) Department of Internal Medicine I, Medical Faculty, RWTH Aachen University, Aachen, Germany
g) Clinical Division and Laboratory of Intensive Care Medicine, Department of Cellular and Molecular Medicine, and Department of Cardiovascular Sciences University Hospital Leuven and KU Leuven, Leuven, Belgium
h) Cardiovascular Research Unit, Department of Precision Health, Luxembourg Institute of Health, Strassen, Luxembourg
i) Hospital General Universitario Gregorio Marañón, Facultad de Medicina, Universidad Complutense de Madrid, Instituto de Investigación Sanitaria Gregorio Marañón, and CIBERCV, Spain
j) Department of Cardiology, Maastricht University, CARIM School for Cardiovascular Diseases, Maastricht, The Netherlands
k) Centre for Molecular and Vascular Biology of Cardiovascular Sciences, KU Leuven, Leuven, Belgium
l) c European Reference Network for Rare, Low Prevalence and Complex Diseases of the Heart (ERN GUARD-Heart)
m) Aix Marseille University, INSERM, INRAE, C2VN, Marseille, France
n. Department of Endocrinology, Metabolic Diseases and Nutrition, APHM, Marseille, France
o) Explorations Fonctionnelles Cardiovasculaires, Hospices Civils de Lyon, 69500 Bron, France
p) Bayer AG, Research & Development, Pharmaceuticals, Wuppertal, Germany
q) Vital-IT group, SIB Swiss Institute of Bioinformatics, Lausanne, Switzerland.
r) Institute of Translational Genomics, Helmholtz Zentrum München, German Research Center for Environmental Health, Neuherberg, Germany
s) Division of Cardiovascular Research, University of Dundee, Scotland, United Kingdom
t) Eli Lilly and Company, Lilly Corporate Center, Indianapolis, IN, United States
u) Boston University Chobanian & Avedisian School of Medicine, Whitaker Cardiovascular Institute, Boston, MA, United States
v) AOU Città della Salute e della Scienza, Medical Genetics Unit, Turin, Italy
† C.D.P and K.S.H contributed equally to this work and share first authorship.
* Corresponding Authors

Abstract:

Background

Diabetic Cardiomyopathy (DiabCM) develops in patients with Type-2-Diabetes Mellitus (T2D) and is characterized by cardiac dysfunction independent of ischemic heart disease or systemic hypertension. Its

underlying mechanisms remain poorly defined with likely genetic and non-genetic mechanisms including epigenetic modifications. Combining T2D-derived polygenic risk scores (PRS) and methylation risk scores (MRS) with key clinical characteristics may aid risk stratification for myocardial dysfunction among patients with T2D.

Methods

We analyzed 173 deeply phenotyped participants from the CARDIATEAM discovery study, grouping them by the severity of myocardial dysfunction determined by echocardiography. Both PRS and MRS show significantly different distribution between severity groups (p-value=0.02 and 1.29e-05, respectively) with significant odds ratios (ORs) at ≥80th and ≥90th percentiles: PRS (2.23 [95%CI 1.03-4.92] and 2.82 [95%CI 1.02-8.34]), and MRS (4.52 [95%CI 2.01-10.83] and 3.49 [95%CI 1.22-11.02]) respectively. Combining individuals with PRS and MRS above the 80th percentile showed a higher OR (6.48). The combined PRS+MRS model demonstrated the best discriminative ability (AUC=0.753), while the interaction model did not enhance performance (AUC=0.752).

Results

Adding PRS and MRS to ten baseline covariates (age, sex and eight cardiometabolic variables) slightly increased bootstrap-validated sensitivity/specificity, from 0.819/0.878 to 0.827/0.885. MRS increased step-wise from non-diabetic low-risk to diabetic high-risk clusters, whereas PRS primarily distinguished diabetic from non-diabetic status. Exploratory pathway analysis of MRS-mapped genes identified enrichment for phosphatase signalling and oxidative-stress pathways implicated in diabetic cardiomyopathy.

Conclusions

This study provides proof-of-concept evidence that integrating T2D-derived polygenic and methylation risk scores with detailed clinical phenotyping captures distinct biological information related to subclinical myocardial dysfunction. MRS showed stronger association, including after adjustment for clinical covariates and in sensitivity analyses restricted to individuals with T2D, whereas the PRS added limited discriminatory

value within the T2D population. These findings are exploratory and require validation in larger independent cohorts.

Research Insights

What is currently known about this topic?	• DiabCM may precede overt HF in T2D patients • Epigenetic changes contribute to diabetic cardiac damage • Early DiabCM biomarkers remain poorly defined
What is the key research question?	Are T2D-derived PRS and MRS associated with subclinical myocardial dysfunction, and do they add information beyond clinical characteristics?
What is new?	• MRS showed a consistent association with subclinical myocardial dysfunction • Combining PRS+MRS slightly improved risk discrimination • Integrated models improved sensitivity and specificity beyond clinical variables
How might this study influence clinical practice?	Multi-omics profiling may support biological characterization of myocardial vulnerability in T2D.

Keywords: Diabetic Cardiomyopathy (DiabCM), Polygenic Risk Score (PRS), Methylation Risk Score (MRS), Type 2 diabetes mellitus (T2D)

List of Abbreviations:

AUC - Area Under the Curve

DiabCM - Diabetic cardiomyopathy

GLS - Global Longitudinal Strain

HbA1c - Glycated Hemoglobin

HF - Heart Failure

MRS - Methylation Risk Score

NMD - No Myocardial Dysfunction

PRS - Polygenic Risk Score

SMD - Subclinical Myocardial Dysfunction

T2D - Type 2 Diabetes Mellitus

Declarations

Ethics approval and consent to participate

The present study was conducted in accordance with the Declaration of Helsinki. The participants provided written informed consent.

Consent for publication:

Not Applicable

Availability of data and materials:

Data that support the findings of this study are available after approval by the Data Access Committee, from the corresponding authors upon request.

Competing interests

CARDIATEAM grant is partnered with Lilly and Bayer. The authors declare no competing financial interests. The authors have reported that they have no relationships relevant to the contents of this paper to disclose.

Funding

This project has received funding from the Innovative Medicines Initiative 2 Joint Undertaking (JU) under grant agreement No 821508. The JU receives support from the European Union’s Horizon 2020 research and innovation programme and EFPIA.

Authors' contributions

KSH and CDP conceptualized and designed the study, performed the analyses, interpreted the data, prepared the figures, and wrote the original draft of the manuscript; they contributed equally to this work

and share first authorship. PB and GAD contributed to clinical data collection. KSH, CDP and EA performed the statistical analyses. RF, MR, AA, SG and AR contributed to laboratory measurements and interpretation. OM provided bioinformatic support. FS, GM and GAD acquired funding. EC, RF, MR, AR, AA, SG, BR, PB , BJ, YD, JB, SH, BG, CB, FS, RL, OM, JLM, MI, EA, RWS, CCL, AND FS contributed to data interpretation and critically revised the manuscript; GM and GAD conceived and supervised the project, and critically revised the manuscript; they share correspondence. All authors read, critically reviewed, and approved the final manuscript.

Acknowledgements

We thank the participants and scientists involved in the CARDIATEAM project for their invaluable contributions to this project.

Authors' information

C.D.P and K.S.H contributed equally to this work and share first authorship.

G.M and G.A.D contributed equally to this study

Background

Type 2 diabetes mellitus (T2D) is expected to impact 578 million people by 2030, making it one of the most common chronic illnesses globally (1). Among its cardiovascular complications, diabetic cardiomyopathy (DiabCM) is a major contributor to heart failure and mortality in patients with T2D, affecting around 17% of the population (2). DiabCM is defined by myocardial dysfunction and remodeling that occurs in the absence of hypertension, coronary artery disease (CAD), and valvular or congenital heart disease. It is increasingly recognized as a distinct multifactorial condition associated with ventricular hypertrophy, impaired myocardial contractility, and complex molecular and cellular alterations (3). However, the precise mechanisms underlying DiabCM remain yet unknown (4),(5).

Cardiac imaging modalities such as echocardiography and cardiac magnetic resonance imaging (CMR) are essential for detecting early subclinical cardiac alteration in T2D before overt cardiomyopathy develops. These methods enable assessment of cardiac function and remodelling, including myocardial fibrosis and microvascular dysfunction (6). Population-based studies have demonstrated increased left ventricular mass (LVM), impaired systolic and diastolic function and increased arterial stiffness in diabetic patients compared with non-diabetic individuals (7). Subtle systolic abnormalities detected by speckle tracking echocardiography (STE) and CMR may precede clinically detectable diastolic dysfunction and the development of overt DiabCM (6). However, these alterations are not unique to T2D, underscoring the need for additional biomarkers to establish the distinctiveness of DiabCM.

Emerging evidence indicates that T2D can induce epigenetic reprogramming of cardiac metabolism, affecting metabolic flexibility and contributing to the development of DiabCM and Heart Failure (HF) (8,9). Although the epigenetic mechanisms involved are not yet fully characterized, DNA methylation represents a promising candidate biomarker due to its dynamic and potentially reversible nature (10). It remains unclear whether integrating epigenetic markers with inherited genetic risk could improve the detection of early, subclinical stages of DiabCM. While current knowledge on epigenetic contributions to DiabCM is limited, emerging studies support their involvement in disease pathogenesis (11). For instance, DNA methylation regulates insulin gene expression, and demethylation of CpG sites in the insulin promoter is crucial for pancreatic β-cell maturation. In parallel, genome-wide association studies indicate that impaired insulin secretion, potentially linked to defects in β-cell development, represents a key initiating mechanism in T2D.

In this study, we explored the contributions of genetic and epigenetic factors to the development of DiabCM prior to symptomatic heart failure. Specifically, we evaluated the relationships between genetic and epigenetic risk scores and the clinical characteristics of individuals with T2D. A Polygenic Risk Score (PRS) summarizes the cumulative contribution of multiple genetic variants associated with disease susceptibility across the genome (12). In contrast, a Methylation Risk Score (MRS) captures changes in methylation patterns across the genome, which can influence disease risk without altering the underlying genetic

sequence (13). While PRS reflects inherited genetic predisposition and remains relatively stable throughout life, MRS represents a more dynamic molecular layer.

Given the stronger and more reproducible evidence supporting T2D-derived genetic and epigenetic risk scores compared with currently unavailable disease-specific DiabCM scores, we adopted a pragmatic strategy using T2D-based molecular signatures as a starting framework. These scores were not designed to capture DiabCM directly; rather, we hypothesized that they may reflect biological heterogeneity among individuals with T2D and help identify those developing early myocardial dysfunction, consistent with previous studies showing that upstream metabolic molecular signatures can stratify downstream disease risk.

We therefore investigated whether integrating T2D-derived PRS and MRS with key clinical characteristics could provide a more comprehensive assessment of DiabCM risk. By capturing both inherited susceptibility and epigenetic modifications, this integrative approach may improve biological characterization of myocardial vulnerability, aiding in patient stratification and guide personalized clinical management strategies.

Materials and methods

Population study

This study included a subset of participants from the CARDIATEAM cohort, a European multicentre longitudinal prospective study conducted across 16 centers in 5 countries. CARDIATEAM recruits patients with and without T2D and performs extensive phenotyping including demographic, metabolic and clinical characteristics. The study is registered on www.clinicaltrials.gov (NCT04303364).

Eligibility participants were consenting women and men aged between 40 and 80 years. All participants were required to have: 1) a normal left ventricular ejection fraction (LVEF ≥ 50%), without akinetic segments on echocardiography; 2) no signs and symptoms of HF; 3) no history of myocardial ischemia, myocardial infarction, percutaneous coronary intervention or coronary artery bypass grafting. Absence of CAD was confirmed by either an absence of coronary stenosis ≥ 50%, a Coronary Artery Calcium (CAC) score <100 on cardiac CT scan or a coronary angiography with a normal Fractional Flow Reserve (FFR >0.80), 48 months prior to inclusion.

T2D diagnosis was defined by medication use, HbA1c ≥ 6.5% and fasting plasma glucose ≥ 7.0 mmol/L. Participants without T2D had an HbA1c <6,5% and fasting plasma glucose <7.0 mmol/L. Individuals with Type 1 diabetes were excluded. Additional exclusion criteria included obstructive and non-obstructive hypertrophic cardiomyopathy (HCM), significant valvular heart disease, chronic atrial fibrillation or significant arrhythmias (premature ventricular contractions, ventricular tachycardia or ventricular fibrillation), severe chronic renal failure (eGFR <30 ml/min/1.73 m^2), life-threatening comorbidities, pregnancy or prior bariatric. Patients with an active COVID-19 infection or prior infection requiring hospitalization were also excluded.

All echocardiographic measurements were centrally evaluated by an independent core laboratory.

Myocardial dysfunction was defined as the presence of at least one of the following criteria previously shown to predict cardiac events in asymptomatic T2D patients (14): E/e' ≥ 13; 3-chamber (3CH-LS) and global longitudinal strain (GLS) < 16%, and LV mass index > 115 g/m2 (males) and > 95 g/m2 (females). Conversely, normal myocardial function was defined by the presence of at least one of the following criteria: E/e' <6.5; 3-chamber (3CH-LS) and global longitudinal strain (GLS) >18.5%, and LV mass index < 95 g/m2 (males) and <90 g/m2 (females).

Among 406 CARDIATEAM participants enrolled between December 2019 to March 2023, 374 individuals with no history of HF, with and without T2D, were included in the present analysis (Supplementary Figure 1). These participants were assigned to clusters using 68 features spanning demographics, clinical symptoms, body measurements, and routine biological parameters. Clustering was performed using self-organizing maps (SOM) based on Kohonen's neural networks (15). Visual inspection of the SOM output, supported by permutation tests for robustness, was used to identify four well contrasted clusters based on clinical and routine biological parameters and echocardiographic features (Supplementary Figure 2, Supplementary Table 1).

Descriptive and univariate analysis

Descriptive statistics were computed to inform clinical, biological, cardiological variables and data availability (missingness rates). Continuous variables were expressed as mean ± standard-deviation or median [interquartile range (IQR)] and categorical variables as counts (percentage). Group comparisons were performed using chi square or Fisher exact tests for categorical variables and one-way ANOVA or Kruskal Wallis tests for continuous variables.

DNA extraction and quality controls

DNA was extracted from buffy-coat recovered from EDTA blood samples (n=179) using the Chemagic DNA Blood 4k magnetic bead extraction kit on the Chemagic™ 360 Instrument (Revvity, USA). DNA integrity was assessed by electrophoresis on E-Gel™ NGS 0.8% agarose gels (Life Technologies, USA), and concentrations were determined fluorometrically with the Qubit™ assay (Thermo Fisher Scientific, USA).

Genotyping analysis

Whole genome genotyping was performed using the Illumina Infinium™ Global Screening Array-24 v3.0 BeadChip (Illumina, USA) following the manufacturer's protocol. Samples, grouped into SMD and NMD, were distributed in a balanced manner across BeadChips, with 24 samples per chip,, for a total of 179 genotyped samples across 8 chips. Arrays were scanned using the iScan System (Illumina, USA) to generate IDAT files.

IDAT files were processed using Genome Studio v2.0.4 with the Illumina Bead Pool Manifest (BPM) and Cluster files and converted into PLINK formats for downstream processing. Quality control procedures excluded 12,677 SNPs with genotype call rate <0.05; 317,486 SNPs with minor allele frequency (MAF) <5%, and 241 SNPs with Hardy-Weinberg exact $p<1e{-}6$. One individual deviating by ±3 standard deviations (SD) from the sample's mean heterozygosity rate was removed. Relatedness was assessed using a pi-hat threshold of 0.125 (i.e., third degree relatives) and one female sample with an X chromosome inbreeding coefficient of 0.37 was excluded. After reference alignment to GRCh38 and variant correction using bcftools +fixref, 292,348 high-quality SNPs and a total of 177 samples remained for imputation. Genotype imputation was performed using the Michigan Imputation Server with the 1000 Genomes Phase 3 reference panel (Version 5) (16),(17). Post-imputation filtering retained variants with imputation quality $R^2>0.8$, yielding 14,056,306 high-confidence SNPs for downstream analyses.

DNA Methylation analysis

Five-hundred nanograms of genomic DNA of 179 samples were bisulfite converted using the EZ-96 DNA Methylation Kit (Zymo Research Corporation, USA). DNA methylation (DNAm) levels were measured using the Infinium MethylationEPIC v2.0 BeadChip (Illumina, USA), following the manufacturer's protocol. Samples were randomly and blindly distributed across the BeadChips and scanned using the iScan System (Illumina, USA).

IDAT files of 177 samples out of 179 were processed using the R-package ChAMP (version 2.29.1) (18). For each CpG locus, methylation levels were expressed as Beta values, calculated as the ratio of methylated signal intensity to the total signal (methylated plus unmethylated), ranging from 0 (no methylation) to 1 (complete methylation). Quality control excluded probes with a detection p-value above 0.01 and samples with more than 10% failed probes. Additional filtering removed probes with a bead count <3 in at least 5% of samples, non-CpG probes, SNP-related probes (19), all multi-hit probes (20) and probes located on chromosome X and Y. After filtering, 853,221 probes remained from the initial 937,055, and 175 samples were retained for further analysis. Data normalization was performed with the «BMIQ» (Beta MIxture Quantile). Singular Value Decomposition (SVD) was applied to the Beta matrix to estimate potential batch effects, which were corrected using “Slide” and “Array” as batch factors. Estimated cell-types proportions were then calculated using EPIDISH based on the Salas’ panel (21). The eight lymphocyte cell types were combined into a single component resulting in five cell components, which were used to adjust normalized methylation Beta values through a linear model.

Risk scores construction

In this study, external weights from the PGS catalog (22) were used to construct the PRS for our samples. PGS values for metabolic disorders, including T2D, were computed using the Michigan Imputation Server. Among 125 available T2D scores (February 2024), 83 were derived from European populations (Supplementary Table 2). We evaluated 36 scores with AUC > 0.6 and Kolmogorov p value < 0.05 for discriminating SMD from NMD. Based on density plots and full variant coverage in our dataset, PGS001357 was selected among available T2D polygenic scores based on its derivation from large European ancestry GWAS meta-analyses, high variant coverage, robust external validation, and compatibility with the ancestry composition of the CARDIATEAM cohort. Scores were generated using PLINK v1.9 (23).

For the MRS, external weights were obtained based on the beta-estimate of 145 CpGs significantly associated with T2D in the Generation Scotland Study (24),(25). More than 80% of these CpG sites were also present in the EWAS catalog (26), after filtering for blood-based studies with a p-value < 3.6e-08 and a sample size > 1000. Due to the different BeadChip used in the Generation Scotland study (Infinium MethylationEPIC v1.0, Illumina), only 134 CpGs overlapped with those measured in our dataset. The MRS was therefore constructed as a linear combination of these 134 CpGs and their corresponding methylation.

PRS-MRS Analysis

Score distributions between SMD and NMD were compared using the Kolmogorov Smirnov test. Logistic regression models were fitted for PRS, MRS, PRS+MRS, and their interaction to evaluate their ability to discriminate groups relative to a base model including age and sex. Model stability was evaluated using bootstrap validation (B=500 resamples) and 10-fold cross-validation. Sensitivity analysis was performed restricted to participants of European ancestry (n=111).

To examine whether higher scores were associated with more severe T2D related cardiomyopathy, Wilcoxon's test was performed after stratifying participants into four groups: Diabetic in SMD, Diabetic in NMD, Non-diabetic in SMD, and Non-diabetic in NMD (Supplementary Table 3). P-values were Benjamini-Hochberg adjusted, with FDR <0.05 considered significant.

PRS and MRS with clinical and echocardiographic characteristics

To assess associations between PRS and MRS with echocardiographic measures of cardiac dysfunction, Spearman correlations were calculated between the scores and available clinical variables. Covariates with missing values were imputed using the missForest algorithm.

We evaluated logistic regression models: base model (adjusted for age and sex), a “covariates” model (base model + selected clinical covariates, described below) and a model incorporating both covariates and risk scores, to check their ability to differentiate the samples with SMD from those with NMD, in particular among the samples with both high genetic and methylation risk scores above the 80th percentile. Odds ratio (OR), Area Under the Curve (AUC), Sensitivity and Specificity were reported to check for the model’s discriminative ability.

From a total of 35 candidate clinical variables (Supplementary Table 4), 13 were excluded prior to modelling as they were components of derived indices already present in the dataset (e.g., weight and height in favour of BMI; waist and hip separately in favour of waist-hip ratio; individual GLS chamber views in favour of composite GLS; unadjusted LAV in favour of BSA-indexed LAV). In the remaining 22 variables, in order to reduce collinearity and redundancy, a feature screening procedure was applied. Each variable was first evaluated using univariate logistic regression, and its coefficient estimate and Wald p value were recorded. Pairwise correlations were then calculated across predictors, and variables with $|r| > 0.25$ were considered correlated. Within each correlated pair, the variable with the stronger univariate association (lower p value)

was retained. This iterative process continued until no correlated predictors remained, resulting in a streamlined set of covariates optimized for predictive relevance and low multicollinearity in multivariable models.

All analyses were conducted using R (version 4.2.2).

Pathway enrichment analysis

The CpGs and SNPs used for the risk score construction were annotated to genes according to the Illumina Infinium MethylationEPIC v2.0 Manifest (27) and VEP (RRID:SCR_002344),(28) respectively. Enrichment analysis was performed using the shinyGO (Gene Ontology Molecular Function) tool, v0.77 (29),(30), and MsigDB (31),(32).

Results

Population description

Clustering analysis of the 374 patients identified four distinct clusters (Supplementary Figure 2) based on clinical, routine biological, and echocardiographic parameters (Supplementary Table 1). Although clustering was not designed to define disease severity, the resulting SOM structure revealed gradients of cardiometabolic burden and functional impairment across clusters. Two clusters (A, female-enriched; B, male-enriched) were predominantly composed of patients with T2D and myocardial dysfunction, whereas clusters C (male-enriched) and D (female-enriched) mainly included individuals without T2D and with normal myocardial function.

From these clusters, two groups were selected for omics analyses after biological sample quality control: 118 patients with subclinical myocardial dysfunction (SMD; 48 females, 70 males; 86 T2D and 32 non-T2D) and 138 patients with no myocardial dysfunction (NMD; 59 females, 79 males; 46 T2D and 92 non-T2D) (Supplementary Table 5). Missing echocardiographic values (<5% of data points) were imputed using the missForest algorithm (33).

Participant inclusion and exclusions after quality control and cardiac function assessment are summarized in Supplementary Table 6. Following biological sample quality control, 179 participants were retained (Supplementary Table 7-8). After data-specific filtering, 175 samples remained in the DNA methylation

dataset (75 SMD, 100 NMD) and 177 in the genotyping dataset (77 SMD, 100 NMD), resulting in a final cohort of 173 individuals with both genotyping and DNA methylation data (Table 1; Supplementary Table 8; Supplementary Figure 1).

These individuals were classified into two omics groups according to cardiac function. The SMD group (n=74) included individuals with echocardiographic evidence of myocardial dysfunction and a higher prevalence of T2D (73%), whereas the NMD group (n=99) included individuals with normal myocardial function and a lower prevalence of T2D (33%). Sex distribution was balanced, with a predominance of males in both groups, and the groups differed clearly in key cardiac parameters (Table 1-2) .

PRS and MRS stratify cardiac dysfunction groups

We derived two risk scores, a PRS from T2D-associated SNPs (PGS001357) and a MRS from T2D-related CpGs. Both scores differed significantly between the groups (PRS: p=0.02; MRS: p=1.29e-05), with the MRS showing the stronger association (Figure 1).

The odds of belonging to the SMD group increased with higher PRS percentiles (>=80th percentile OR=2.23, 95%CI 1.03-4.92, p=0.04; >=90th percentile OR=2.82, 95%CI 1.02-8.34, p=0.05). Adding PRS to the base model including age and sex did not significantly improve discrimination over the base model alone (AUC 0.64 to 0.67; DeLong p=0.3) (Figure 2).

The MRS showed a high discriminative ability (AUC 0.75; DeLong p=0.04 vs PRS AUC 0.67). Individuals above the 80th percentile had significantly higher odds of SMD (OR=4.52, 95%CI 2.01-10.83; p=0.0004). At the 90th percentile (SMD=12, NMD=6), the OR was 3.49 (95%CI 1.22-11.02; p=0.02), with approximately 70% belonging to the SMD group. Sensitivity and specificity were 0.41 and 0.77 for PRS alone, and 0.43 and 0.79 for MRS alone.

We next evaluated models including both scores and their interaction. The combined PRS+MRS model achieved an AUC of 0.753 for distinguishing SMD from NMD (DeLong p=0.04 vs base model AUC=0.64), whereas including the interaction term did not improve performance (Figure 2). To assess model stability, bootstrap validation (B=500) confirmed no evidence of overfitting (bootstrap mean AUC=0.765, 95% CI 0.689-0.839, and 10-fold cross-validation yielded a mean CV-AUC of 0.743 (SD=0.126), closely consistent with the observed AUC. Nagelkerke pseudo R2 indicated greater variance explained for models including both scores compared with those including either score alone (Table 3). Individuals with both PRS and

MRS above the 80th percentile had markedly higher odds of SMD (OR=6.48), with sensitivity and specificity of 0.47 and 0.82, respectively.

In a sensitivity analysis restricted to European-ancestry participants (n=111), results were consistent with the primary analysis. The combined PRS+MRS model achieved AUC=0.787 (bootstrap mean 0.804, 95% CI 0.720-0.876,10-fold CV-AUC=0.835). In this ancestry-restricted sensitivity analysis, both scores contributed independently (PRS OR=1.79 [1.12-3.02]; MRS OR=2.34 [1.40-4.24]), and the combined model significantly outperformed the base model (DeLong p=0.029).

Stratification by diabetes status

Importantly, the inclusion of individuals with T2D in both SMD and NMD groups was intentional, as it allowed us to investigate heterogeneity in myocardial vulnerability within diabetes rather than simply contrasting diabetic versus non-diabetic status. Because the presence of T2D across both SMD and NMD groups was central to our study design, we further explored score distributions within diabetic subgroups to determine whether molecular risk scores could distinguish diabetic individuals with versus without subclinical myocardial dysfunction.

MRS gradually increased from non-diabetic individuals in NMD (mean 16.6) and SMD (mean 16.9), to diabetic individuals in SMD (mean 18.05) with intermediate values in diabetic individuals in NMD (mean 17.53) (Figure 3A). The significant difference between diabetic in SMD and those in NMD (FDR-adjusted p-value = 0.011) supports the potential value of MRS in capturing biological heterogeneity and myocardial vulnerability among individuals with T2D.

In contrast, PRS values were similar between diabetic individuals in SMD (mean 7.24e-08) and NMD (mean 7.48e-08) , but both groups showed higher PRS compared with non-diabetic individuals in NMD (mean 4.87e-08) (FDR-adjusted p = 0.0007) (Figure 3B).

Because T2D prevalence differed between the SMD and NMD groups, we additionally adjusted for T2D status and related metabolic characteristics; the MRS remained associated with SMD after adjustment for

T2D status, HbA1c, and waist-to-hip ratio (OR per 1-SD increase = 1.71, 95% CI 1.10-2.74, p = 0.016), whereas the PRS was not associated with SMD (OR = 1.00, p = 0.98).

Additionally, as a direct empirical test of discrimination within the diabetic population alone, we performed a sensitivity analysis restricted to participants with T2D (n=87; SMD=54, NMD=33). Using Firth penalised logistic regression adjusting for age, sex, HbA1c, and waist-to-hip ratio, the MRS remained associated with SMD (OR per 1-SD increase = 1.80, 95% CI 1.11-3.12, p = 0.016).

The PRS remained unassociated with SMD within T2D patients (OR=0.94, p=0.97), consistent with the primary analysis.

PRS and MRS correlation with clinical and biological traits

The Spearman's correlation tests highlighted significant correlations with some clinical and biological traits. MRS was significantly correlated with anthropometric indicators of adiposity, including weight, BMI, waist and hip circumference, as well as fasting glycemia, HbA1c, and triglyceride levels, consistent with its derivation from a T2D-associated methylation signature. MRS was also associated with higher high-sensitivity troponin T (hs-TnT), indicating subclinical myocardial injury. PRS correlated positively with waist circumference, waist-to-hip ratio, fasting glucose and HbA1c (Figure 5A,5B).

PRS and MRS correlation with echocardiographic parameters

The correlation tests also highlighted significant correlation with critical cardiac parameters for both PRS and MRS (Figures 4A, 4B).

Cardiac geometry: MRS positively correlated with end-diastolic septal wall thickness (EDSWT) and end-diastolic posterior wall thickness (EDPWT). PRS showed a negative association with left-ventricular end-diastolic diameter (LVEDD).

Systolic function: MRS was positively associated with global longitudinal strain (GLS) in 4-chamber, 2-chamber, and 3-chamber views, and with mid-level global circumferential strain (GCS-mid), whereas higher PRS values were associated with lower absolute GLS values.

Diastolic function: Higher MRS values correlated negatively with E/A ratio, septal and lateral E′ velocities, and left atrial strain (LA-LS res), while positively correlating with conduit-phase left atrial strain (LA-LS conduit). PRS showed inverse correlations with lateral and septal E′, and left-atrial reservoir strain.

In predictive models, 22 candidate covariates were screened by univariate logistic regression and pairwise Pearson correlation (|r| > 0.25), yielding eight variables (Supplementary Table 9). Feature reduction was applied exclusively to limit overparameterization and improve model stability in relation to sample size, rather than to replace clinically informed confounder adjustment. A multivariate model incorporating the selected clinical covariates (Waist-hip ratio, Triglycerides, Fasting glycemia, Fasting HbA1c, hs-TnT, EA, E-mean, Left Atrial Volume (LAV Simpson)), achieved a bootstrap-validated sensitivity of 0.819 (95% CI 0.705-0.911) and specificity of 0.878 (95% CI 0.812-0.935). Adding PRS and MRS to this model yielded sensitivity of 0.827 (95% CI 0.702-0.918) and specificity of 0.885 (95% CI 0.813-0.941).

Exploratory enrichment analysis of PRS- and MRS-mapped genes

Annotation of the 134 CpG sites used to construct the MRS mapped to 111 genes. Pathway over-representation analysis revealed significant enrichment for phosphatidylinositol-4-phosphate phosphatase activity (Enrichment FDR = 0.03). In contrast, the 2,141,165 SNPs underlying the PRS mapped to 8,069 genes but showed no significant pathway enrichment after multiple-testing correction The CpG and SNP derived gene lists overlapped at 23 protein coding genes (Supplementary Table 10). A hypergeometric test against a background of 32,973 protein-coding genes annotated in the Illumina Infinium MethylationEPIC v2.0 manifest confirmed that this overlap does not exceed chance expectation (expected=27.2, fold enrichment=0.85, p=0.85). Exploratory pathway analysis of the 23 overlapping genes identified associations with AMP-deaminase (34), hydrolase, phosphoric-ester hydrolase and phosphatase activities (Supplementary Table 11) (35),(36),(37).

MSigDB enrichment analyses identified four FDR-significant gene-set signatures (Supplementary Table 12). The NFE2L2.V2 (FDR=9.6×10^{-3}), E2F3_UP.V1_DN cell-cycle signature (FDR=9.6×10^{-3}), TLR4/NF-κB signalling in macrophages (FDR=1.9×10^{-2}) and $CD34^{+}$ progenitor-cell signature (FDR=3.4×10^{-2}).

Several cranio-facial phenotype terms also reached significance; their relevance to the cardiac phenotype is uncertain.

Discussion

To our knowledge, this is the first study to examine, within the same individuals, how a T2D-derived PRS and MRS jointly relate to subclinical myocardial dysfunction and early cardiac remodeling. Our findings indicate that MRS was more closely associated with subclinical myocardial dysfunction than the PRS, which primarily reflected inherited susceptibility to T2D. Although integrating these molecular layers resulted in only modest improvements in predictive discrimination, the findings support the concept that genetic and epigenetic information capture complementary aspects of disease biology beyond what conventional clinical variables alone provide. The clinical relevance of the observed performance requires external validation.

Although both scores were derived from T2D-related datasets, they contributed differently to the cardiac phenotype. Both PRS and MRS were significantly higher in individuals with SMD, but MRS showed a better discriminative ability (AUC 0.75), while PRS exhibited poorer discrimination, attenuated when adjusting for HbA1c, and adiposity. Notably, individuals above the 80th percentile for both scores exhibited 6.5-fold higher odds of belonging to the SMD group compared with the remainder of the cohort. However, confidence intervals remained wide owing to the limited sample size, and this finding should therefore be interpreted cautiously until confirmed in larger independent cohorts.

The combined model was largely driven by the stronger association of the MRS with myocardial dysfunction, whereas the PRS contributed complementary information regarding inherited susceptibility to T2D. This likely reflects the distinct biological roles of the two molecular layers, with DNA methylation representing cumulative metabolic exposure and myocardial remodelling, while inherited genetic variation reflects baseline disease susceptibility.

When stratifying the cohort according to diabetic status and cardiac phenotype, a clear gradient emerged for the MRS. Values increased progressively from non-diabetic individuals without dysfunction to diabetic

individuals with subclinical myocardial dysfunction, suggesting that the MRS may reflect cumulative metabolic exposure together with myocardial remodelling, thereby capturing the biological heterogeneity associated with early myocardial dysfunction in T2D. In contrast, the PRS was elevated in all diabetic patients relative to the non-diabetic participants but did not differentiate between diabetics with and without myocardial dysfunction. The only significant contrasts occurred between each diabetic subgroup (Diabetic in SMD and in NMD) and the non-diabetic individuals in NMD. This dissociation was confirmed in a sensitivity analysis restricted to participants with T2D, where the MRS remained independently associated with SMD while the PRS did not. These findings suggest that PRS primarily reflects inherited predisposition to T2D itself rather than the degree of myocardial involvement and supports a dual-layer architecture in which genetic predisposition reflects diabetes susceptibility, which is consistent with its original design.

By contrast, methylation changes may capture diabetes-related myocardial remodelling, consistent with the concept that epigenetic variation reflects cumulative metabolic exposure together with ongoing myocardial remodelling. These subgroup findings should be interpreted as preliminary biological evidence rather than definitive proof of diabetic cardiomyopathy-specific risk stratification. The limited number of diabetic participants precludes robust development of a clinically applicable prediction model restricted to T2D alone, and larger dedicated cohorts will be required for this purpose.

Consistent with this interpretation, Spearman correlation analysis confirmed that both scores track clinically relevant phenotypes. The MRS demonstrated strong associations with both metabolic and cardiac functional parameters. Its positive correlation with markers of adiposity, glycemic control, and triglycerides underscores its relevance to cardiometabolic risk. Moreover, significant associations with echocardiographic indicators of left ventricular hypertrophy, impaired myocardial strain, and impaired diastolic function highlight its potential to capture early subclinical cardiac remodeling. The inverse correlations with NT-proBNP, mitral annular velocities, and atrial strain further support a link between elevated MRS and diastolic dysfunction.

The PRS, on the other hand, showed a narrower but coherent pattern. It aligns with central adiposity, hyperglycaemia and a subtly adverse functional pattern, lower absolute GLS values and lower diastolic velocities (latE′, SeptE′), while being inversely related to NT-proBNP. This profile is consistent with inherited

T2D susceptibility accompanied by an adverse cardiometabolic phenotype, although the cross-sectional correlations do not establish that the PRS directly contributes to cardiac impairment. Taken together, the PRS and MRS capture complementary, yet partially overlapping, biological dimensions associated with cardiometabolic risk and myocardial remodelling, although they do not establish a diabetic cardiomyopathy-specific epigenetic signature.

From a predictive standpoint, a small set of 8 clinical, biochemical, and echocardiographic covariates were independently informative and increased diagnostic sensitivity and specificity to 0.827 and 0.885 respectively when integrated with both the scores respectively. These modest improvements indicate that the genetic and epigenetic scores capture pathophysiological information that is only partially reflected in standard clinical variables and that the principal value of integrating PRS and MRS in this study lies in improving biological characterization of disease heterogeneity rather than providing an immediately applicable clinical prediction tool.

At the molecular level, while the overlap between PRS- and MRS-mapped genes did not exceed chance expectation, exploratory pathway analysis of the MRS-mapped genes identified significant enrichment for phosphatidylinositol-4-phosphate phosphatase activity, consistent with biological processes previously implicated in diabetic cardiomyopathy, although these exploratory analyses do not establish mechanistic relationships. Among the overlapping genes, AMPD3 (adenosine monophosphate deaminase 3) and several phosphatases (including PTPRU, LHPP, INPP5F) were noted, with MSigDB analysis pointing to signatures related to oxidative-stress defence (NRF2), cell-cycle regulation (E2F3), innate-immune activation (TLR4/NF-κB), and progenitor-cell biology, all previously implicated in the pathogenesis of DiabCM (38),(39),(40),(41). These observations are hypothesis-generating and do not establish mechanistic relationships.

Mechanistically, AMPD3 hyperactivity at endoplasmic reticulum-mitochondria contact sites has been linked to mitochondrial Ca2+ overload and impaired energy production, contributing to cardiac dysfunction (34). In parallel, increased activity of protein phosphatases such as PP1 and PP2A disrupts calcium cycling and sarcoplasmic reticulum function, promoting early systolic and diastolic impairment (36). Protective

mechanisms involving Nrf2-mediated antioxidant pathways have also been described, highlighting oxidative stress and mitochondrial dysfunction as central processes in DiabCM (35),(37).

Overall, our findings support the hypothesis that integrating inherited genetic susceptibility with dynamic epigenetic information may improve biological characterization of individuals at risk of diabetic myocardial dysfunction. Whether such a layered strategy provides clinically meaningful benefit will require validation in larger independent cohorts.

Study Limitations

Several limitations should be acknowledged. First, the discovery cohort comprised 173 individuals, a sample size appropriate for a deeply phenotyped multi-omic discovery study, but smaller than what is typically required to establish robust risk prediction models. This is consistent with comparable multi-omic cardiology studies in similarly well-characterised cohorts, yet confidence intervals around odds ratios remain wide and findings should be considered hypothesis-generating pending larger-scale replication. The relatively small sample size together with the study design may limit generalizability, although all the patients are being actively followed longitudinally for additional major clinical events. Consequently, the MRS may partly reflect disease-associated epigenetic changes because it was derived from affected individuals. Moreover, methylation was measured in whole blood rather than cardiac tissue. While blood-based methylation is the only feasible approach in large-scale clinical studies, it may not fully recapitulate the cardiac epigenome. Although cardiac tissue analysis may provide a more precise representation of established myocardial pathology, it is inherently less accessible and often reflects later-stage disease. By contrast, peripheral blood may capture earlier systemic and metabolic alterations that precede overt cardiac remodeling, making it a pragmatic substrate for prospective biomarker development.

The biological relevance of blood-derived methylation signatures for myocardial phenotypes cannot be assumed directly, although the consistent and directionally coherent associations observed in our data, together with prior literature linking circulating epigenetic marks to cardiovascular outcomes, support their potential translational relevance.

Moreover, some potentially relevant factors, particularly diabetes duration and medication exposure, may still contribute to residual confounding; comprehensive adjustment for all such factors was not statistically feasible given the sample size without substantial risk of overfitting. An additional limitation relates to the origin of the molecular risk scores used in this study. Both PRS and MRS were derived from T2D-associated datasets rather than from diabetic cardiomyopathy-specific discovery cohorts. While this approach allowed us to test whether upstream diabetes-related molecular liability could identify individuals with early myocardial dysfunction, it limits disease specificity. The development of diabetic cardiomyopathy-specific polygenic and methylation risk scores will require larger, deeply phenotyped cohorts and independent validation datasets, which are not yet available.

External validation in an independent cohort was therefore not possible due to the lack of similarly deep phenotyped datasets integrating multi-omic and echocardiographic data and remains an important next step within the broader CARDIATEAM project, which is currently recruiting a larger confirmatory cohort. Finally, because both scores were derived and tested in a predominantly European population, their transferability to other ancestries remains uncertain and will require validation with ancestry matched scores in diverse, non-European populations (42–44).

Conclusions

These findings provide a rationale for evaluating a layered molecular and clinical strategy in future studies of asymptomatic individuals with T2D. Among the two molecular layers evaluated, the MRS showed a more consistent association with subclinical myocardial dysfunction, whereas the PRS primarily reflected inherited susceptibility to T2D. Polygenic risk profiling is stable across the life course and could, in principle, be assessed at or before diagnosis, whereas methylation-based measures may provide more dynamic information as metabolic abnormalities accumulate. Whether such a layered approach can distinguish individuals with T2D who develop cardiomyopathy from those who do not requires prospective evaluation in independent cohorts. These findings provide a basis for future work to develop and validate diabetic cardiomyopathy-specific molecular risk scores.

Additional Files

Supplementary material is available in Supplemental_Appendix.docx

Figure legends:

Figure 1: Performance of polygenic and methylation risk scores. (A) Boxplots showing the distribution of PRS and (B) MRS by SMD/NMD status. Density plots illustrating differences in the distributions of PRS (C) and MRS (D) between SMD and NMD.
Figure 2: Receiver Operating Characteristic (ROC) curves comparing model performance in distinguishing SMD from NMD: base model (blue, AUC=0.64), PRS model (purple, AUC=0.67), MRS model (orange, AUC=0.75), combined model (green, AUC=0.75), and interaction model (red, AUC=0.75).

Figure 3: Boxplots showing the distribution of (A) Methylation Risk Score (MRS) and (B) Polygenic Risk Score (PRS) across four subgroups: diabetic SMD, diabetic NMD, non-diabetic SMD, and non-diabetic NMD. Scores are shown on the y-axis, with significant differences indicated by FDR-adjusted p-values.

Figure 4A: Pair-wise correlation matrix for 35 clinical and echocardiographic variables in the CARDIATEAM discovery cohort. Colours encode the Spearman coefficient (ρ): deep blue = strong positive (+1), white = no correlation (0), deep red = strong negative (–1). Black asterisks mark correlations that remain significant at P<0.05 after false-discovery-rate correction.
Figure 4B: Focused view of the two omic scores: methylation risk score (MRS) and polygenic risk score (PRS), against the clinical covariates.
Figure 4 Abbreviations: BMI, body-mass index; NT-proBNP, N-terminal pro-brain natriuretic peptide; hs-TnT, high-sensitivity troponin T; EDSWT/EDPWT, end-diastolic septal/posterior wall thickness; GLS, global longitudinal strain (4CH, 2CH, 3CH views); GCS, global circumferential strain (basal, mid ventricular, apical); LA-LS, left-atrial longitudinal strain (res = reservoir, conduit); LVEDD/LVEDV, left-ventricular end-diastolic diameter/volume; LAV-ES, left-atrial volume at end-systole (Simpson method, BSA-indexed); E_mean, early-diastolic transmitral flow velocity; lat E′ / sept E′, lateral/septal mitral-annular early-diastolic velocity; LVM, left-ventricular mass.

Tables

Table 1: Baseline characteristics of the 173 participants in the CARDIATEAM discovery cohort, stratified by cardiac dysfunction group.

Characteristic	Missing (%)	Overall N = 173[1]	SMD N=74[1]	NMD N=99[1]	p-value[2]
General features					
Age, yeas	0	59.9 ±7.6	61.9 ±7.6	58.8 ±7.3	0.002
Female sex	0	73 (42.2%)	32 (43.2%)	41 (41.4%)	0.81
Inclusion criteria					

T2D	0				<0.001
No T2D AND no HFpEF		86 (49.7%)	20 (27.0%)	66 (66.7%)	
T2D AND no HFpEF		87 (50.3%)	54 (73.0%)	33 (33.3%)	
Addictive behavior					
Alcohol consumption	0	98 (56.6%)	42 (56.8%)	56 (56.6%)	0.98
Other addictive behaviors	0	2 (1.2%)	1 (1.4%)	1 (1.0%)	0.84
Smoking	0				0.76
Active smoker		26 (15.0%)	11 (14.9%)	15 (15.2%)	
Former smoker		42 (24.3%)	20 (27.0%)	22 (22.2%)	
No		105 (60.7%)	43 (58.1%)	62 (62.6%)	
Personal disease history					
Diabetic feet - History	7	0 (0.0%)	0 (0.0%)	0 (0.0%)	>0.99
Diabetic neuropathy	7	9 (5.4%)	7 (9.5%)	2 (2.2%)	0.079
Microalbuminuria	7	16 (9.6%)	10 (13.5%)	6 (6.5%)	0.13
Retinopathy	7	14 (8.4%)	7 (9.5%)	7 (7.6%)	0.67
Diabetes duration (years)	89	13.9 [9.3;19.0]	13.7 [10.3;19.6]	14.1 [7.5;18.4]	0.54
Body composition and Physical examination					
Lean mass (%)	69	63.3 [56.6;67.5]	58.9 [53.8;64.8]	65.3 [60.3;69.1]	0.007
Fat mass (%)	38	33.0 [27.6;39.7]	36.1 [31.0;42.0]	30.7 [25.8;35.3]	<0.001
Diastolic blood pressure, mmHg	2	78.4 ±10.6	80.9 ±11.8	76.5 ±9.2	0.009
Systolic blood pressure, mmHg	2	131 [121;143]	140 [126;150]	129 [117;139]	<0.001
Heart rate, bpm	1	67.0 [60.0;79.0]	76.0 [66.0;81.0]	65.0 [57.0;70.0]	<0.001
Height, cm	1	169 ±10.1	168 ±9.3	169 ±10.7	0.60
Weight, kg	1	80.1 ±16.1	86.1 ±14.5	75.6 ±15.8	<0.001
BMI, kg/m^2	1	27.4 [24.4;31.5]	30.5 [27.2;33.3]	25.4 [23.1;28.5]	<0.001
Waist, cm	53	97.0 [89.0;107]	102 [95.0;114]	94.0 [82.0;102]	<0.001

Hip, cm	53	103 [96.0;111]	106 [100;111]	98.0 [92.0;110]	<0.001
Waist-to-Hip-ratio	53	0.96 [0.89;1.01]	0.97 [0.91;1.02]	0.95 [0.86;0.99]	0.074
Waist/Height	53	0.58 [0.52;0.63]	0.61 [0.57;0.66]	0.55 [0.50;0.60]	<0.001
Biological parameters					
Fasting glycemia, mmol/L	11	5.7 [5.1;7.8]	6.6 [5.5;8.9]	5.4 [4.90;6.5]	<0.001
Fasting HbA1c, %	15	6.1 [5.6;7.4]	7.0 [6.1;8.0]	5.7 [5.4;6.6]	<0.001
hsTnT, ng/L	30	5.0 [3.00;8.0]	5.5 [3.90;10.1]	5.0 [3.00;7.0]	0.034
LDH, U/L	16	177 [153;202]	175 [150;200]	179 [155;203]	0.41
NT-proBNP, ng/L	10	42.0 [20.0;80.0]	42.5 [20.0;83.0]	42.0 [20.0;74.0]	0.85
us-CRP, mg/L	27	1.85 [0.80;4.00]	2.30 [1.00;4.00]	1.10 [0.60;4.00]	0.043
ALAT, U/L	8	27.0 [20.0;37.0]	28.0 [21.0;35.0]	25.0 [19.0;39.0]	0.22
ALP, U/L	13	73.0 [60.0;87.5]	73.5 [62.0;95.0]	72.5 [58.0;85.0]	0.28
ASAT, U/L	49	23.5 [19.0;27.5]	24.0 [20.0;30.0]	23.0 [19.0;27.0]	0.25
CPK, U/L	42	110 [78.0;163]	104 [78.0;164]	116 [82.0;159]	0.48
γ-GT, U/L	11	25.0 [19.0;37.0]	26.5 [21.0;38.5]	23.5 [19.0;33.0]	0.023
Fasting insulinemia, µIU/mL	36	9.0 [5.8;14.0]	11.0 [7.6;17.9]	7.6 [5.1;12.4]	0.003
Creatinine, µmol/L	10	73.0 [60.0;85.0]	72.0 [60.0;89.0]	73.5 [62.5;83.0]	0.98
eGFR, mL/min/1.73 m^2	20	86.0 [60.0;91.0]	82.5 [60.0;90.0]	87.0 [67.0;93.0]	0.22
Albumin to creatinine ratio, mg/mmol	115	1.20 [0.10;4.20]	0.90 [0.10;4.20]	1.40 [0.10;6.6]	0.58
Cholesterol total, mmol/L	11	4.49 [3.70;5.2]	4.02 [3.30;4.90]	4.71 [4.00;5.3]	<0.001
LDLc total, mmol/L	10	2.65 [1.92;3.31]	2.20 [1.77;2.85]	2.98 [2.29;3.48]	<0.001

HDLc total, mmol/L	10	1.30 [1.09;1.60]	1.20 [1.04;1.50]	1.31 [1.10;1.66]	0.13
Triglycerides total, mmol/L	11	1.10 [0.80;1.49]	1.28 [0.90;1.50]	1.00 [0.70;1.47]	0.008
Cardiac report, Cardiac strain and ETT					
LVEF (%)	2	62.0 [57.0;64.0]	62.0 [57.0;65.0]	62.0 [57.0;64.0]	0.96
LAESVI, mL/m^2	10	31.2 [26.9;38.9]	30.9 [26.0;37.2]	32.4 [28.1;40.2]	0.06
LVEDV, mL	2	116 [95.0;142]	116 [90.0;143]	114 [97.0;142]	0.99
LVESV, mL	2	44.0 [34.0;57.0]	44.0 [34.0;60.0]	45.5 [36.0;57.0]	0.91
LVEDD, cm	0	4.77 ±0.59	4.82 ±0.68	4.74 ±0.52	0.39
E, m/s	0	0.68 [0.59;0.79]	0.62 [0.54;0.74]	0.73 [0.63;0.82]	<0.001
A, m/s	0	0.73 [0.61;0.84]	0.79 [0.70;0.88]	0.68 [0.57;0.78]	<0.001
E/A	0	0.94 [0.78;1.10]	0.78 [0.70;0.91]	1.06 [0.96;1.21]	<0.001
Deceleration time, ms	0	194 [168;227]	200 [176;239]	188 [161;213]	0.004
latE', cm/s	0	11.0 [9.0;13.0]	9.0 [8.0;10.0]	12.0 [11.0;14.0]	<0.001
septE', cm/s	0	8.0 [7.0;10.0]	7.0 [6.0;8.0]	10.0 [8.0;11.0]	<0.001
E/e' mean	0	7.0 [5.8;8.7]	8.0 [6.4;9.8]	6.2 [5.4;7.9]	<0.001
E/e'mean ≥ 13 (n, %)	0	1 (0.6%)	1 (1.4%)	0 (0.0%)	0.43
E/e'mean < 6.5 (n, %)	0	71 (41%)	21 (28.4%)	50 (50.5%)	0.003
LA-LS-conduit, %	12	-15.0 [-18.0;-11.0]	-12.0 [-15.0;-9.0]	-17.0 [-20.0;-14.0]	<0.001
LA-LS-contract, %	12	-16.0 [-18.0;-14.0]	-17.0 [-19.0;-14.0]	-15.0 [-17.0;-13.0]	0.024
LA-LS-res, %	12	30.0 [27.0;34.0]	27.5 [25.0;32.0]	31.0 [28.0;36.0]	<0.001
TR Vmax, m/s	58	2.40 [2.20;2.60]	2.39 [2.22;2.63]	2.40 [2.16;2.57]	0.68

EDPWT, cm	0	0.80 [0.70;1.00]	0.90 [0.80;1.00]	0.80 [0.70;0.90]	0.002
EDSWT, cm	0	0.90 [0.80;1.00]	1.00 [0.90;1.10]	0.90 [0.70;1.00]	<0.001
GLS (absolute value, %)	0	18.9 [17.2;20.7]	17.3 [16.4;19.6]	19.6 [18.4;21.7]	<0.001
GLS < 16% (n, %)	0	19 (11%)	14 (18.9%)	5 (5.1%)	0.004
GLS > 18.5% (n, %)	0	93 (53.8%)	23 (31.1%)	70 (70.7%)	<0.001
2CH-LS (absolute value, %)	0	19.2 [17.5;21.5]	17.9 [16.3;19.5]	20.4 [18.7;22.5]	<0.001
4CH-LS (absolute value, %)	0	18.9 [17.4;20.9]	18.2 [16.3;19.3]	19.4 [17.8;21.5]	<0.001
3CH-LS (absolute value, %)	0	18.6 [16.7;20.3]	17.0 [14.9;19.0]	19.5 [18.1;20.8]	<0.001
3CH-LS < 16% (n, %)	0	34 (19.7%)	27 (36.5%)	7 (7.1%)	<0.001
3CH-LS > 18.5% (n, %)	0	87 (50.3%)	22 (29.7%)	65 (65.7%)	<0.001
LVMi (g/m2)	1	84.2 [67.8;104]	93.2 [73.1;106]	78.9 [66.7;99.2]	0.010
LVMi, g/m² (Categorical)	30				0.001
Male: LVMi <95 g/m2		51 (35.7%)	19 (30.2%)	32 (40%)	
Female: LVMi<95 g/m2		55 (38.5%)	18 (28.6%)	37 (46.3%)	
Male: LVMi >115 g/m2		21 (14.7%)	13 (20.6%)	8 (10%)	
Female: LVMi >95 g/m2		16 (11.2%)	13 (20.6%)	3 (3.8%)	
H/R^3	0	0.36 [0.30;0.41]	0.38 [0.32;0.42]	0.34 [0.30;0.39]	0.023
IV and Confounding factors					
Geographic origin	2				0.42
Europe		112 (65.5%)	47 (63.5%)	65 (67.0%)	
Northern Africa		27 (15.8%)	14 (18.9%)	13 (13.4%)	
Africa		11 (6.4%)	7 (9.5%)	4 (4.1%)	
Afro-American		1 (0.6%)	1 (1.4%)	0 (0.0%)	
Asian		4 (2.3%)	1 (1.4%)	3 (3.1%)	
India / Pakistan / Bangladesh		3 (1.8%)	1 (1.4%)	2 (2.1%)	

South America	3 (1.8%)	1 (1.4%)	2 (2.1%)
West Indies	10 (5.8%)	2 (1.1%)	8 (8.1%)

[1]Mean ±SD; n (%); Median [Q1;Q3]

[2]Welch Two Sample t-test; Pearson's Chi-squared test; Fisher's exact test; Wilcoxon rank sum test

[3]H/R = (2 * EDPWT)/LVEDD

https://www.sciencedirect.com/science/article/pii/S0735109715074094#:~:text=Relative%20wall%20thickness%20(RWT)%2C%20defined%20as%202,diastolic%20diameter%2C%20is%20a%20measure%20of%20LV

Table 2. Echocardiographic features according to the two groups , stratified by cardiac dysfunction, undergoing omics analysis (N = 173).

Characteristic	SMD N=74[1]	NMD N=99[1]	p-value[2]
E/e' mean >= 13	1 (1.4%)	0 (0.0%)	0.25
E/e'lat >= 13	1 (1.4%)	0 (0.0%)	0.25
e'lat < 10	43 (58.1%)	10 (10.1%)	<0.001
LAESVI Simpson > 34 ml/m2	23 (33.8%)	45 (47.4%)	0.084
3CH-LS absolute < 16%	27 (36.5%)	7 (7.1%)	<0.001

[1]n (%)

[2]Pearson's Chi-squared test

Table 3. Cragg-Uhler R^2 values across models for all markers

Model	**Cragg–Uhler R^2**
Combined	0.220
Interaction	0.224
MRS	0.211

PRS	0.112

Figures

Figure 1: Performance of polygenic and methylation risk scores. (A) Boxplots showing the distribution of PRS and (B) MRS by SMD/NMD status. Density plots illustrating differences in the distributions of PRS (C) and MRS (D) between SMD and NMD.

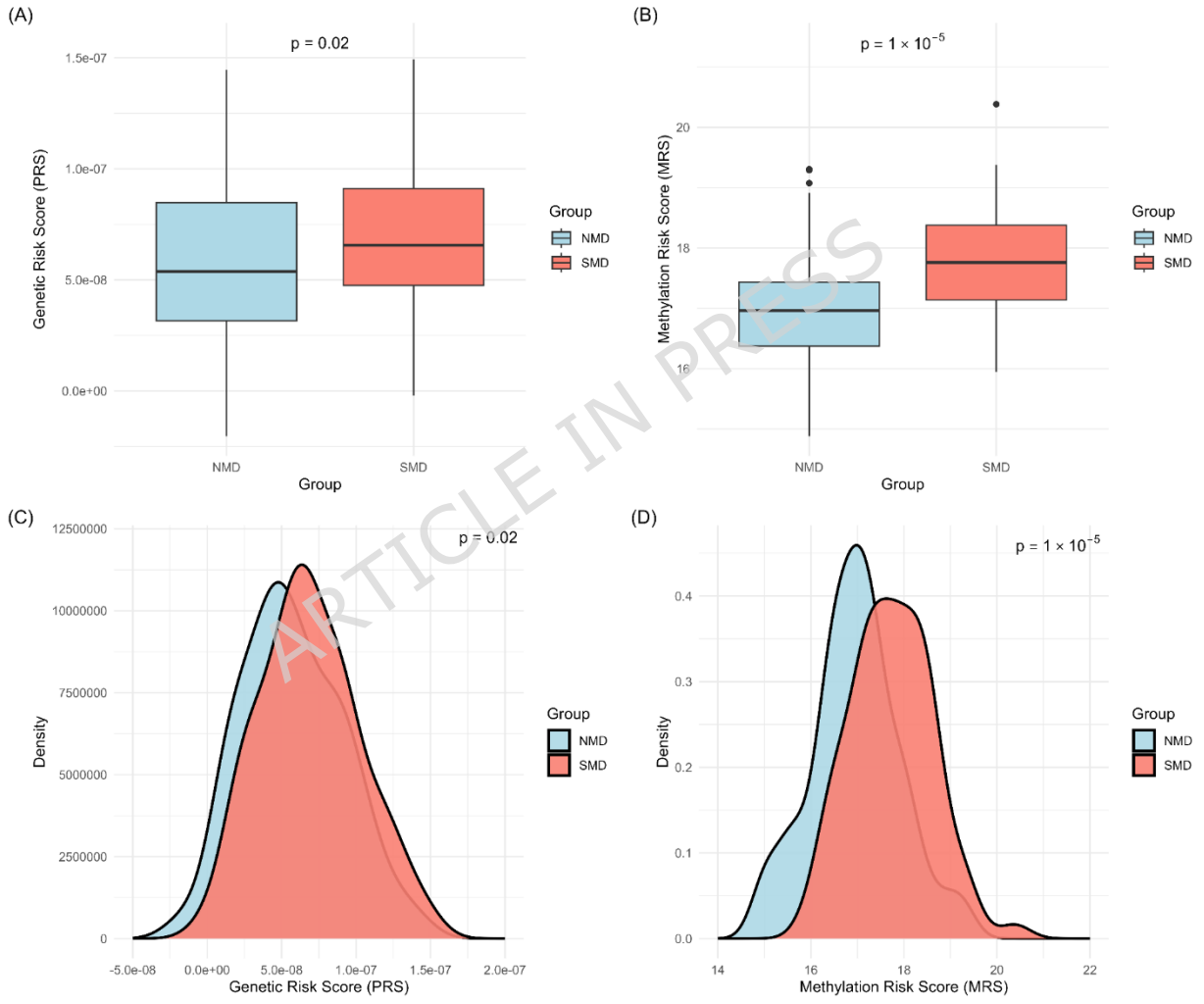

Figure 2: Receiver Operating Characteristic (ROC) curves comparing model performance in distinguishing SMD from NMD: base model (blue, AUC=0.64), PRS model (purple, AUC=0.67), MRS model (orange, AUC=0.75), combined model (green, AUC=0.75), and interaction model (red, AUC=0.75).

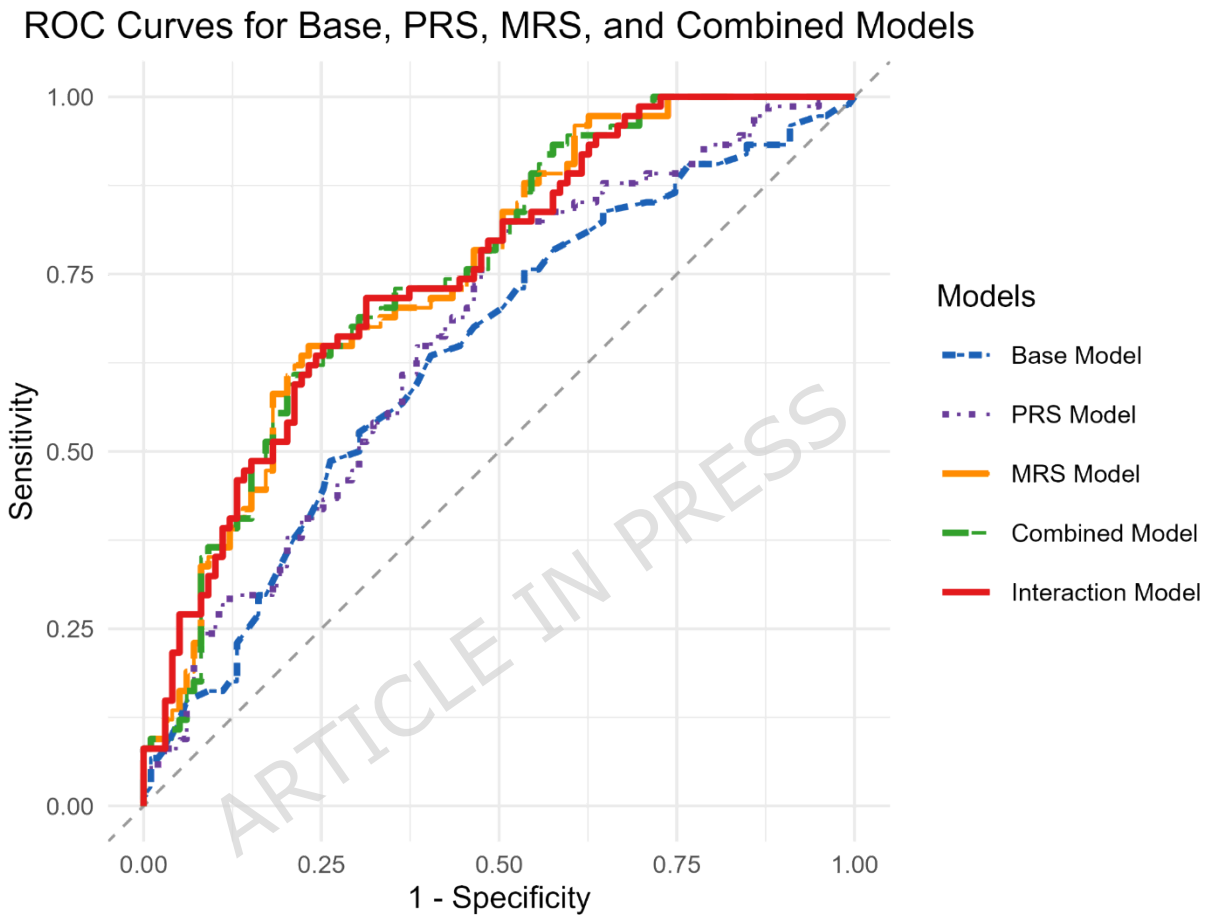

Figure 3: Boxplots showing the distribution of (A) Methylation Risk Score (MRS) and (B) Polygenic Risk Score (PRS) across four subgroups: diabetic SMD, diabetic NMD, non-diabetic SMD, and non-diabetic NMD. Scores are shown on the y-axis, with significant differences indicated by FDR-adjusted p-values.

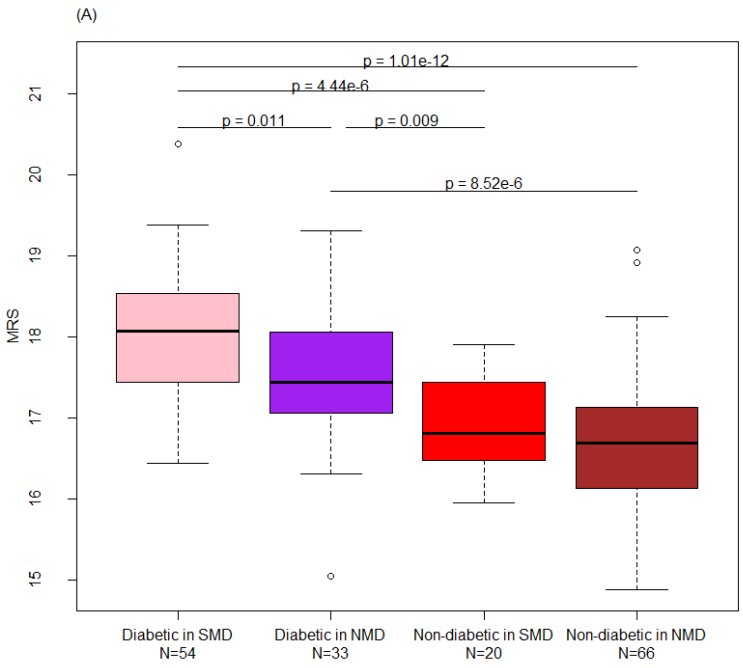

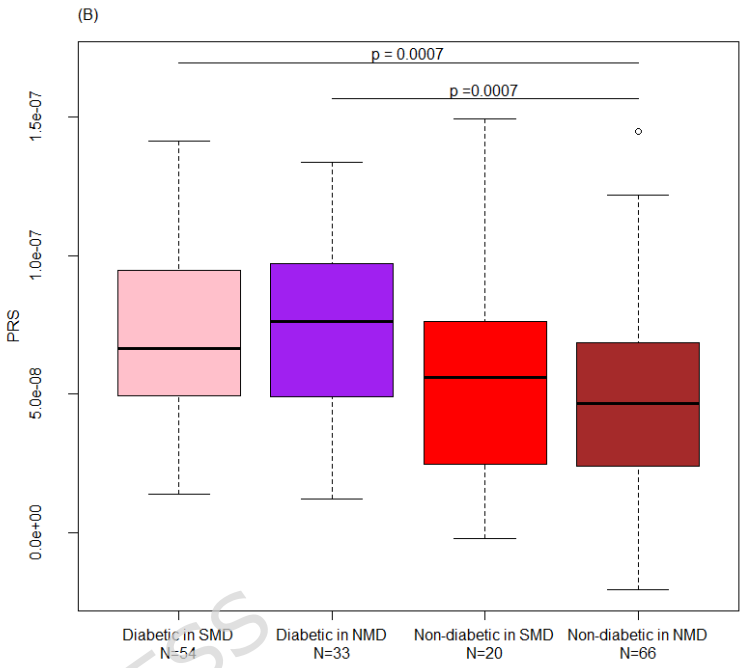

Figure 4A: Pair-wise correlation matrix for 35 clinical and echocardiographic variables in the CARDIATEAM discovery cohort. Colours encode the Spearman coefficient (ρ): deep blue = strong positive (+1), white = no correlation (0), deep red = strong negative (–1). Black asterisks mark correlations that remain significant at P<0.05 after false-discovery-rate correction.

Figure 4B: Focused view of the two omic scores: methylation risk score (MRS) and polygenic risk score (PRS), against the clinical covariates.

Figure 4 Abbreviations: BMI, body-mass index; NT-proBNP, N-terminal pro-brain natriuretic peptide; hs-TnT, high-sensitivity troponin T; EDSWT/EDPWT, end-diastolic septal/posterior wall thickness; GLS, global longitudinal strain (4CH, 2CH, 3CH views); GCS, global circumferential strain (basal, mid ventricular, apical); LA-LS, left-atrial longitudinal strain (res = reservoir, conduit); LVEDD/LVEDV, left-ventricular end-diastolic diameter/volume; LAV-ES, left-atrial volume at end-systole (Simpson method, BSA-indexed); E_mean, early-diastolic transmitral flow velocity; lat E′ / sept E′, lateral/septal mitral-annular early-diastolic velocity; LVM, left-ventricular mass.

(A)

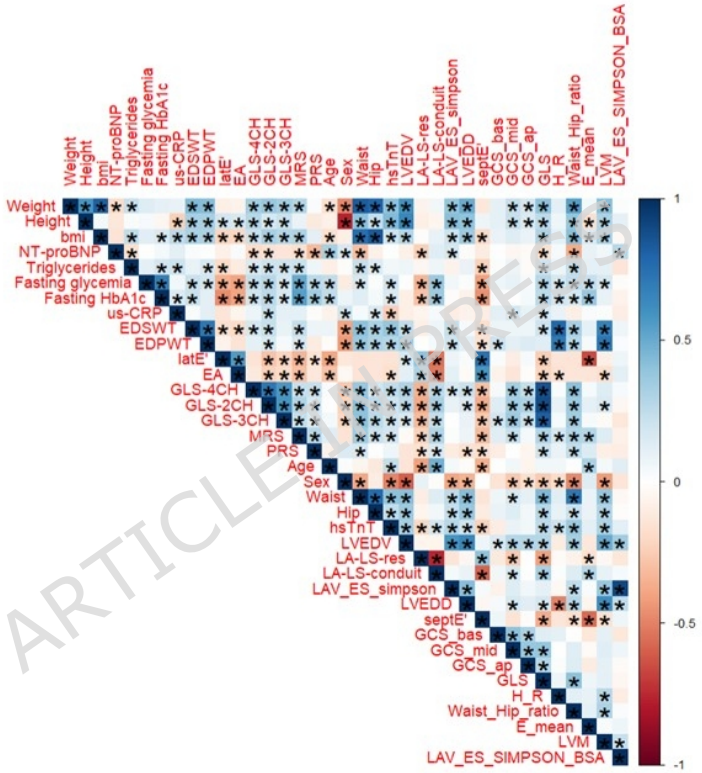

(B)

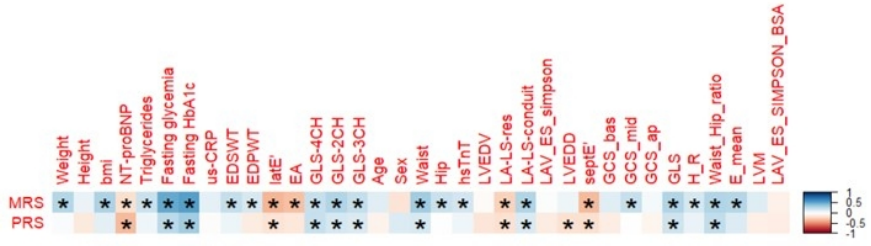

References

1. Saeedi P, Petersohn I, Salpea P, Malanda B, Karuranga S, Unwin N, et al. Global and regional diabetes prevalence estimates for 2019 and projections for 2030 and 2045: Results from the International Diabetes Federation Diabetes Atlas, 9 edition. Diabetes Res Clin Pract. 2019 Nov;157:107843.

2. Zygmunciak P, Stróżna K, Błażowska O, Mrozikiewicz-Rakowska B. Extracellular Vesicles in Diabetic Cardiomyopathy—State of the Art and Future Perspectives. International Journal of Molecular Sciences. 2024 Jun 1;25(11):6117.

3. Rubler S, Dlugash J, Yuceoglu YZ, Kumral T, Branwood AW, Grishman A. New type of cardiomyopathy associated with diabetic glomerulosclerosis. Am J Cardiol. 1972 Nov 8;30(6):595–602.

4. Tan Y, Zhang Z, Zheng C, Wintergerst KA, Keller BB, Cai L. Mechanisms of diabetic cardiomyopathy and potential therapeutic strategies: preclinical and clinical evidence. Nat Rev Cardiol. 2020 Sep;17(9):585–607.

5. Zygmunciak P, Stróżna K, Błażowska O, Mrozikiewicz-Rakowska B. Extracellular Vesicles in Diabetic Cardiomyopathy—State of the Art and Future Perspectives. International Journal of Molecular Sciences. 2024 Jun 1;25(11):6117.

6. Marwick TH, Gimelli A, Plein S, Bax JJ, Charron P, Delgado V, et al. Multimodality imaging approach to left ventricular dysfunction in diabetes: an expert consensus document from the European Association of Cardiovascular Imaging. Eur Heart J Cardiovasc Imaging. 2022 Jan 24;23(2):e62–84.

7. Devereux RB, Roman MJ, Paranicas M, O'Grady MJ, Lee ET, Welty TK, et al. Impact of diabetes on cardiac structure and function: the strong heart study. Circulation. 2000 May 16;101(19):2271–6.

8. Cooper ME, El-Osta A. Epigenetics: mechanisms and implications for diabetic complications. Circ Res. 2010 Dec 10;107(12):1403–13.

9. Russell-Hallinan A, Karuna N, Lezoualc'h F, Matullo G, Baker H, Bernard M, et al. Established and Emerging Roles of Epigenetic Regulation in Diabetic Cardiomyopathy. Diabetes Metab Res Rev. 2025 Sep;41(6):e70081.

10. Targeting epigenetics in diabetic cardiomyopathy: Therapeutic potential of flavonoids. Biomedicine & Pharmacotherapy. 2023 Jan 1;157:114025.

11. Zheng J, Cheng J, Zhang Q, Xiao X. Novel insights into DNA methylation and its critical implications in diabetic vascular complications. Biosci Rep. 2017 Mar 15;37(2):BSR20160611.

12. Choi SW, Mak TSH, O'Reilly PF. Tutorial: a guide to performing polygenic risk score analyses. Nature Protocols. 2020 Jul 24;15(9):2759–72.

13. Hüls A, Czamara D. Methodological challenges in constructing DNA methylation risk scores. Epigenetics. 2020 Jan-Feb;15(1-2):1–11.

14. Wang Y, Yang H, Huynh Q, Nolan M, Negishi K, Marwick TH. Diagnosis of Nonischemic Stage B Heart Failure in Type 2 Diabetes Mellitus: Optimal Parameters for Prediction of Heart Failure. JACC Cardiovasc Imaging. 2018 Oct;11(10):1390–400.

15. The self-organizing map [Internet]. [cited 2025 Aug 8]. Available from: http://dx.doi.org/10.1109/5.58325

16. 1000 Genomes Project Consortium, Auton A, Brooks LD, Durbin RM, Garrison EP, Kang HM, et al. A global reference for human genetic variation. Nature. 2015 Oct 1;526(7571):68–74.

17. Das S, Forer L, Schönherr S, Sidore C, Locke AE, Kwong A, et al. Next-generation genotype

imputation service and methods. Nat Genet. 2016 Oct;48(10):1284–7.

18. Tian Y, Morris TJ, Webster AP, Yang Z, Beck S, Feber A, et al. The Chip Analysis Methylation Pipeline [Internet]. 2025 [cited 2025 Aug 8]. Available from: https://www.bioconductor.org/packages/devel/bioc/vignettes/ChAMP/inst/doc/ChAMP.html

19. Zhou W, Laird PW, Shen H. Comprehensive characterization, annotation and innovative use of Infinium DNA methylation BeadChip probes. Nucleic Acids Res. 2017 Feb 28;45(4):e22.

20. Nordlund J, Bäcklin CL, Wahlberg P, Busche S, Berglund EC, Eloranta ML, et al. Genome-wide signatures of differential DNA methylation in pediatric acute lymphoblastic leukemia. Genome Biology. 2013 Sep 24;14(9):1–15.

21. Salas LA, Koestler DC, Butler RA, Hansen HM, Wiencke JK, Kelsey KT, et al. An optimized library for reference-based deconvolution of whole-blood biospecimens assayed using the Illumina HumanMethylationEPIC BeadArray. Genome Biology. 2018 May 29;19(1):1–14.

22. Lambert SA, Gil L, Jupp S, Ritchie SC, Xu Y, Buniello A, et al. The Polygenic Score Catalog as an open database for reproducibility and systematic evaluation. Nat Genet. 2021 Apr;53(4):420–5.

23. Purcell S, Neale B, Todd-Brown K, Thomas L, Ferreira MAR, Bender D, et al. PLINK: a tool set for whole-genome association and population-based linkage analyses. Am J Hum Genet. 2007 Sep;81(3):559–75.

24. Cheng Y, Gadd DA, Gieger C, Monterrubio-Gómez K, Zhang Y, Berta I, et al. Development and validation of DNA methylation scores in two European cohorts augment 10-year risk prediction of type 2 diabetes. Nat Aging. 2023 Apr;3(4):450–8.

25. Generation Scotland [Internet]. [cited 2025 Aug 8]. Generation Scotland. Available from: https://genscot.ed.ac.uk/node/50073

26. MRC-IEU EWAS Catalog [Internet]. [cited 2025 Aug 8]. Available from: https://www.ewascatalog.org/

27. Infinium MethylationEPIC v2.0 Product Files [Internet]. [cited 2025 Aug 8]. Available from: https://support.illumina.com/downloads/infinium-methylationepic-v2-0-product-files.html

28. McLaren W, Gil L, Hunt SE, Riat HS, Ritchie GRS, Thormann A, et al. The Ensembl Variant Effect Predictor. Genome Biol. 2016 Jun 6;17(1):122.

29. ShinyGO 0.77 [Internet]. [cited 2025 Aug 8]. Available from: https://bioinformatics.sdstate.edu/go77/

30. Ge SX, Jung D, Yao R. ShinyGO: a graphical gene-set enrichment tool for animals and plants. Bioinformatics. 2019 Dec 27;36(8):2628–9.

31. Subramanian A, Tamayo P, Mootha VK, Mukherjee S, Ebert BL, Gillette MA, et al. Gene set enrichment analysis: A knowledge-based approach for interpreting genome-wide expression profiles. Proceedings of the National Academy of Sciences. 2005 Oct 25;102(43):15545–50.

32. Liberzon A, Birger C, Thorvaldsdóttir H, Ghandi M, Mesirov JP, Tamayo P. The Molecular Signatures Database (MSigDB) hallmark gene set collection. Cell Syst. 2015 Dec 23;1(6):417–25.

33. Stekhoven DJ, Bühlmann P. MissForest--non-parametric missing value imputation for mixed-type data. Bioinformatics (Oxford, England) [Internet]. 2012 Jan 1 [cited 2026 Feb 3];28(1). Available from: https://pubmed.ncbi.nlm.nih.gov/22039212/

34. Osanami A, Sato T, Toda Y, Shimizu M, Kuno A, Kouzu H, et al. Adenosine monophosphate deaminase in the endoplasmic reticulum–mitochondria interface promotes mitochondrial Ca2+ overload in type 2 diabetes rat hearts. Journal of Diabetes Investigation. 2023 Apr 1;14(4):560–9.

35. Fang Q, Liu X, Ding J, Zhang Z, Chen G, Du T, et al. Soluble Epoxide Hydrolase Inhibition Protected against Diabetic Cardiomyopathy through Inducing Autophagy and Reducing Apoptosis Relying on Nrf2 Upregulation and Transcription Activation. Oxid Med Cell Longev. 2022 Mar 25;2022:3773415.

36. Elevated levels of protein phosphatase 1 and phosphatase 2A may contribute to cardiac dysfunction in diabetes. Biochimica et Biophysica Acta (BBA) - Molecular Basis of Disease. 2003 Jul 30;1638(3):273–7.

37. Wang Y, Zhang Y, Chen K, Liu J, Wu D, Cheng Y, et al. Insufficient S-adenosylhomocysteine hydrolase compromises the beneficial effect of diabetic BMSCs on diabetic cardiomyopathy. Stem Cell Res Ther. 2022 Aug 13;13(1):418.

38. Chen J, Zhang Z, Cai L. Diabetic Cardiomyopathy and Its Prevention by Nrf2: Current Status. Diabetes & Metabolism Journal. 2014 Oct 17;38(5):337.

39. Xu Q, Chen X, Zhao C, Liu Y, Wang J, Ao X, et al. Cell cycle arrest of cardiomyocytes in the context of cardiac regeneration. Front Cardiovasc Med. 2025 Apr 28;12:1538546.

40. Dong B, Qi D, Yang L, Huang Y, Xiao X, Tai N, et al. TLR4 regulates cardiac lipid accumulation and diabetic heart disease in the nonobese diabetic mouse model of type 1 diabetes. Am J Physiol Heart Circ Physiol. 2012 Sep 15;303(6):H732–42.

41. Huang G, Cheng Z, Hildebrand A, Wang C, Cimini M, Roy R, et al. Diabetes impairs cardioprotective function of endothelial progenitor cell-derived extracellular vesicles via H3K9Ac inhibition. Theranostics. 2022 May 21;12(9):4415–30.

42. Martin AR, Kanai M, Kamatani Y, Okada Y, Neale BM, Daly MJ. Clinical use of current polygenic risk scores may exacerbate health disparities. Nat Genet. 2019 Apr;51(4):584–91.

43. Kengne AP, Amoah AGB, Mbanya JC. Cardiovascular Complications of Diabetes Mellitus in Sub-Saharan Africa. Circulation [Internet]. 2005 Dec 6 [cited 2025 Aug 8]; Available from: https://www.ahajournals.org/doi/10.1161/CIRCULATIONAHA.105.544312

44. Paiman EHM, van Eyk HJ, Bizino MB, Dekkers IA, de Heer P, Smit JWA, et al. Phenotyping diabetic cardiomyopathy in Europeans and South Asians. Cardiovasc Diabetol. 2019 Oct 11;18(1):133.